Available online at www.sciencedirect.com

Science Direct

materialstoday: PROCEEDINGS

[iCEE 2k19]

Chrysin mediated synthesis, crystallographic structure and optical emission characteristics of ZnO nanoparticles

Praveen K. H.[1] and Arun S. Prasad[2]*

[1]*Post Graduate Department of Physics, S. N. College, Chengannur, Alappuzha-689508, Kerala, India*
[2]*Post Graduate Department of Physics, TKMM College, Nangiarkulangara, Alappuzha-690513, Kerala, India*
**Corresponding author, email: asp.physics@gmail.com*

Abstract

ZnO nanoparticles were synthesized through chrysin mediated phytochemical reduction mechanism. pH of the reaction mixture was kept proximate to 9 and the reaction was carried out at room temperature. The powdered sample obtained was annealed at 600 ^{o}C for four hours. X-ray diffraction pattern analysis revealed the formation of nanocrystalline hexagonal primitive lattice phase of zinc (II) oxide with crystallite size equal to16 nm as estimated from Debye-Scherrer equation. The coalescence resulted from annealing the sample which led to the formation of needle like grains of edge to edge crystallites aggregate was evidenced from FESEM images, with grain size equivalent to crystallite size calculated from x-ray diffraction analysis. Tauc' plot of uv-visible spectrum employing Kubelka-Munk function provided a direct optical band gap of 3.27 eV. The photoluminescence spectrum using 280 nm optimal excitation wavelength and the related color coordinates estimated from chromaticity diagram revealed that the optical emission in the sample occurs at blue region in the visible spectrum.

Keywords: Nanocrystalline, Phytochemicals, Chrysin, Kubelka-Munk function, photoluminescence etc;

1. Introduction

Zinc (II) oxide (ZnO) nanoparticles have been attracted intense attention over the years, especially because of their photocatalytic [1], optoelectronic device [2] and solar cell [3] applications. The high efficiency, low cost and non-toxicity altogether brought this semiconducting material as a promising candidate for device fabrication in connection with light harnessing [4]. Due to the interesting physical properties, for instance the larger absorption coefficient, high carrier mobility and high chemical stability, ZnO has been listed as a well known gas sensing material as well [4]. In analogy with our earlier reports [5-8] on phytochemical mediated synthesis of various semiconducting transition metal oxide nanostructures such as Fe_2O_3 [5, 6], Mn_3O_4 [7] CuO [8], an attempt has been made to synthesis ZnO nanostructures using phytochemical mediated reduction method.

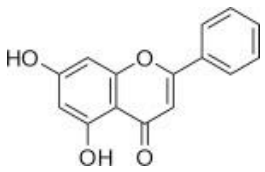

Fig. 1. Molecular structure formula of the natural flavonoid chrysin (5, 7 - dihydroxy - 2 –phenyl – 4H – chromen – 4 - one) [9]

Chrysin has been used as phytochemical mediator. Figure 1 shows the molecular structure formula of the natural

"Peer-review under responsibility of the scientific committee of the International Conference on Energy and Environment", iCEE 2k19, 12-14th December 2019, T.K.M. College of Arts Science, Karicode, Kollam 691005, Kerala, India.

flavonoid chrysin (5, 7 - dihydroxy - 2 –phenyl – 4H – chromen – 4 - one) [9]. Recently, chrysin has been identified as a potential candidate for inhibiting aromatase and human immune deficiency virus activation [9]. It has also been demonstrated as having superior anti inflammatory effects and has shown capability as antioxidants [9]. The chemo preventive activity of chrysin was explored for utility in cancer treatment in a variety of human and rat cells [9]. Natural existence of chrysin is found to be rich in honey and propolis [10]. In this context, this paper reports the detailed analysis on crystallographic structure, morphological features, band gap evaluation and emission characteristics of ZnO nanostructures synthesized through chrysin mediated chemical reduction method.

2. Experimental

The precursor salt, zinc sulfate hepta hydrate ($ZnSO_4.7H_2O$) was purchased from Merck Life Science Pvt. Ltd. and used without further purification. Aqueous solution of 0.1M precursor was mixed with 0.0125M alkaline solution of Chrysin dissolved in 1M NaOH solution by keeping 2:3 volume ratio. The mixture was stirred at room temperature for 1 hr and the pH was regularly tested and maintained at 7 to 8. The change in color to a pale yellowish during the course of reaction was indicative of the reduction reaction being carried out. The mixture was then kept in dark for an overnight to settle down and the solid residue obtained was separated using whatman filter paper. The filtrate was then washed a number of times using de-ionized water to confiscate all the adhering impurities. The filtrate was then dried in air and crushed into fine powders before put in the crucible for annealing at 600 ^oC for 4 hrs. The sample is here after referred to as Zn-NP-CHRYN. Various analytical results obtained after characteristic measurements such as XRD, FESEM, uv-visible spectroscopy and photoluminescence studies have been discussed.

3. Results and discussion

3.1. X-ray diffraction measurement

Figure 2 shows the indexed XRD pattern recorded for Zn-NP-CHRYN powder sample at SICC, Kariyavattom Campus, University of Kerala, Thiruvananthapuram, Kerala, India. BRUKER D8 ADVANCE diffractometer system with 280 goniometer radius was used for the measurement. An x-ray wavelength of 1.5406 Å was allowed to impinge on the sample in scan angle, 2θ ranging from 10° to 90° in 0.020348 step size [7].

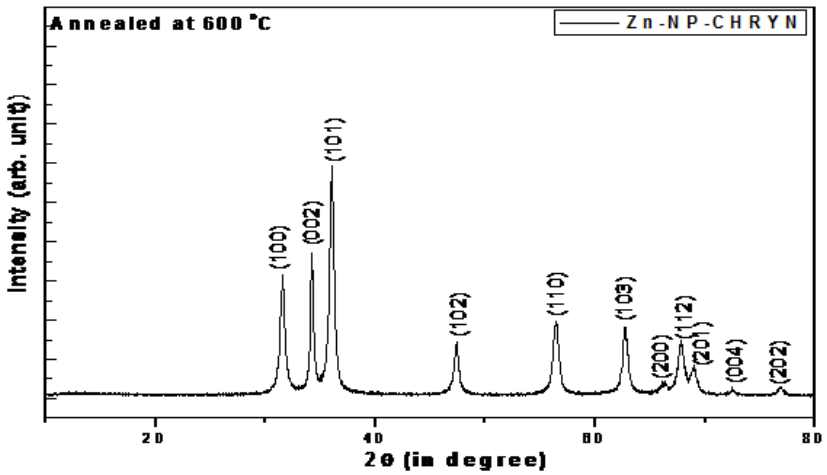

Fig. 2. XRD pattern recorded for Zn-NP-CHRYN sample

The Bragg reflection peaks with crystallographic planes corresponding to hexagonal primitive lattice of Zinc (II) oxide (ZnO) phase was obtained in consistent with the report in JCPDS: ICDD PCPDFWIN #PDF Number: 89-1397 under the space group P63mc (186), which implies that Zn-NP-CHRYN samples were crystallized in single phase alone without having any impurity content. Table 1 gives the list of parameters obtained after crystallographic

study.

Significant broadening in peaks in the x-ray reflection lines indicates the formation of nanocrystalline structure. The crystallite size was evaluated using Debye-Scherrer equation [11]:

$$t = \frac{0.9\lambda}{\beta \cos\theta_B} \qquad (1)$$

Where t is the thickness of the particle, the x-ray wavelength (λ) is equal to 1.5406 Å, β is the full width at half maximum (FWHM) of the main peak under consideration and θ_B is the Bragg angle of reflection. The FWHM is calculated from figure 3, which represents Gauss fit corresponding to most intense (101) Bragg' reflection peak in the XRD pattern. The obtained value of FWHM is 0.49604^0. The crystallite size was thus estimated to be 16 nm.

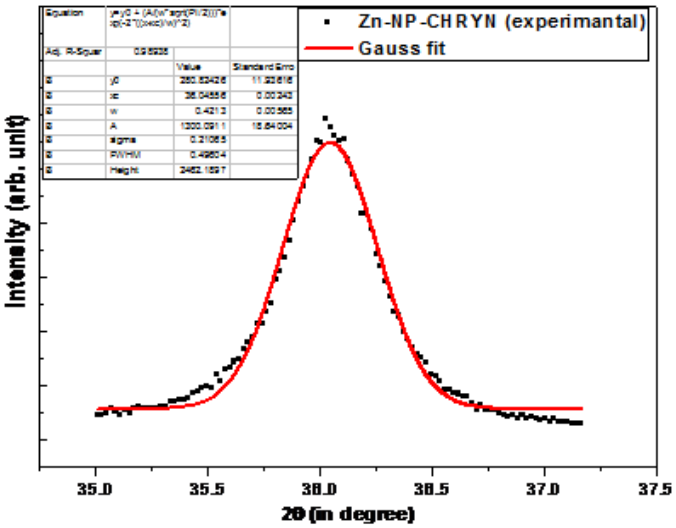

Fig. 3. Gauss fit corresponding to (101) Bragg' reflection peak in the XRD pattern

Table 1. List cell parameters and crystallite size (using Scherer equation) for Zn-NP-CHRYN sample estimated from XRD patterns

Sample Name	Cell parameter (lattice constant)			Crystallite size, *t* (nm)
	a(Å)	*b*(Å)	*c*(Å)	
	From JCPDS	*From JCPDS*	*From JCPDS*	
ZnO (Chrysine)	3.253	--	5.213	16

3.2. FESEM analysis

The desirable properties for gas-sensing application such as the large surface to volume ratio and high porosity have been exhibited by ZnO nanostructures [4]. In order for enhancing the gas-sensing property, ZnO nanostructures with various morphologies are promising [4]. It is thus reasonable to test the morphological topography of ZnO synthesized by chrysin mediated phytochemical reduction method as well. The morphological structures of ZnO depend on the growth parameters of *pH*, time, temperature and the precursors used. The Field Emission Scanning Electron Microscope (FESEM) patterns recorded for various magnifications such as 50,000x, 1,00,000x, 1,50,000x and 2,00,000x for Zn-NP-CHRYN samples, using Nova NanoSEM 450 device installed at Department of Optoelectronics, University of Kerala, Kariyavattam Campus, Thiruvananthapuram, Kerala, India is shown in figure 4. It is obvious from the images that the sample is composed of needle like grains with average cylindrical diameter

equal to 16 nm. This grains size is in well agreement with the crystallite size calculated from XRD pattern using Debye-Scherrer equation. During the course of annealing, the nucleated crystallites grow into certain characteristic shapes and coalesce with the neighboring ones by rounding off their edges near the joining neck region, where the crystallites assume a molten liquid like structure. The coalescence involves considerable transfer of mass between the nucleated crystallites by diffusion. Small crystallites disappear rapidly. Thus during the process of annealing the coalescence causes re-crystallization through the crystallite necks, leading to some definite shapes of larger masses called grains. Depending on the mode of assembling of crystallites's aggregate into grains, distinct morphological features could be explored using FESEM imaging. The Zn-NP-CHRYN sample under investigation here shows needle like grain morphology with average size equal to the average crystallite size. This is attributed to the edge to -

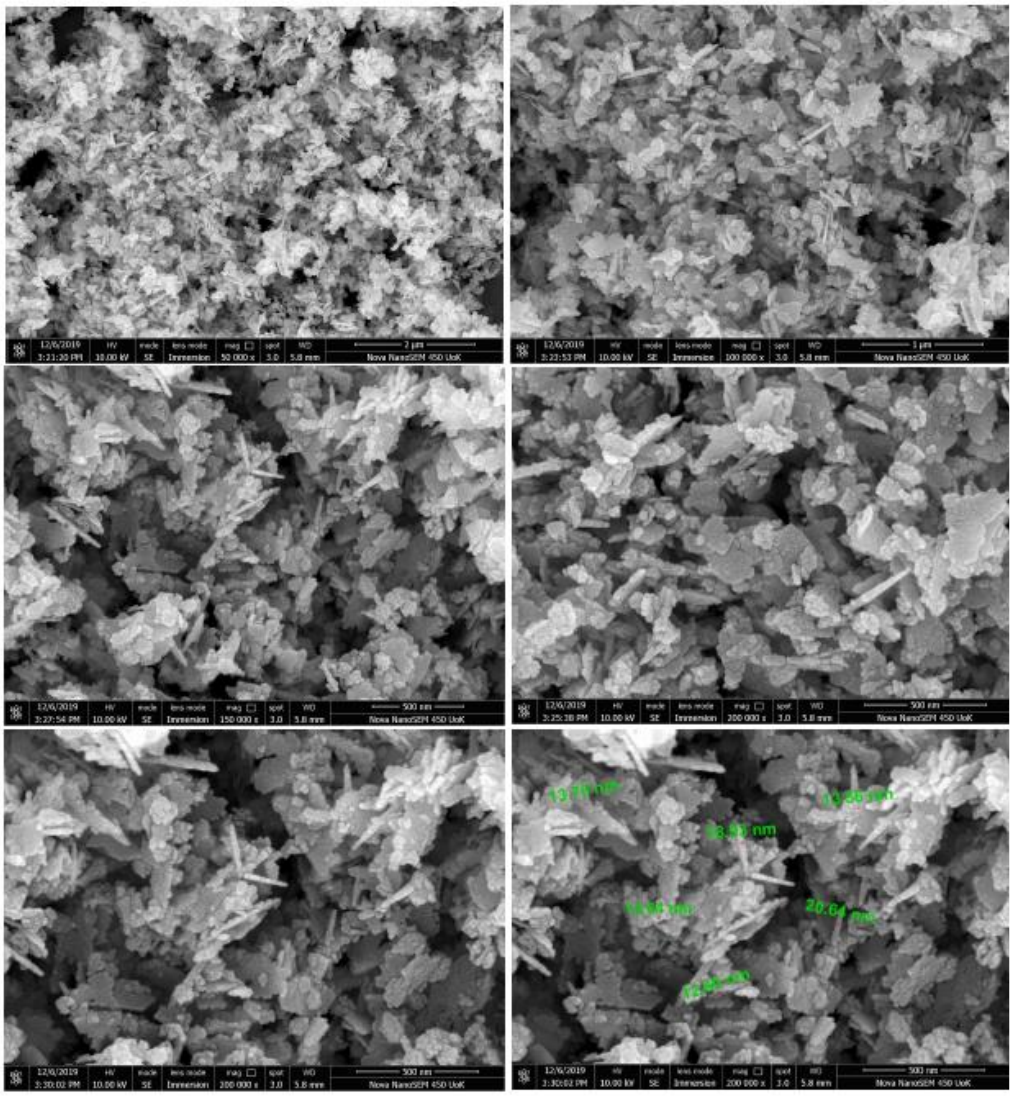

Fig. 4. FESEM inages obtained for Zn-NP-CHRYN at different magnifications

edge coalescence of crystallites through linear aggregation alone. In fact, in addition to the earlier said factors, the selection of phytochemical component as well plays a momentous role in deciding the rate of nucleation of crystallites and mode of aggregation yielding to different grains morphology.

3.3. Uv-visible spectrum analysis

The uv-visible spectrum was recorded in reflectance mode at Department of Physics, University of Kerala, Kariyavattom campus, Thiruvananthapuram, Kerala, India. From the reflectance spectrum, Kubelka-Munk equation is calculated as [12]:

$$F(R) = \frac{(1-R)^2}{2R} = \frac{k}{s} \qquad (2)$$

where k is the molar absorption coefficient and s is the scattering factor. From equation (2), it is apparent that $F(R)$ is relative to absorption coefficient of the sample and hence is the significant parameter in deciding the semiconducting efficacy, nature and band gap energy.

Further, the band gap is estimated from the following expression using Kubelka-Munk function, proposed by Mott, Davis and Tauc [13-15]:

$$F(R)h\nu = A\,(h\nu - E_g)^n \qquad (3)$$

Where hν is the photon energy, E_g is the optical energy gap situated between the localized states near the mobility edges according to the density of states model proposed by Mott and Davis [7,15] and A is the characteristic parameter independent of photon energy, sometimes called band tailing parameter [7]. In equation (3) there is another constant (n), known as the power factor of transition mode [7]. The value of power factor, say n = 2 stands for indirect allowed transition, n = 3 for indirect forbidden transition, n = 1/2 for direct allowed transition and n = 3/2 for direct forbidden transition [7].

The uv-visible spectrum recorded in reflection mode for Zn-NP-CHRYN sample is depicted in figure 5. For perfectly crystalline transition metal oxides, direct band gap would be higher compared to indirect band gap [14]. Accordingly, the data have been plotted for both direct and indirect allowed transition modes. The inset of figure 5 shows the modified Tauc's plot [13-15] employing Kubelka-Munk function [12] corresponding to direct (n=1/2; $(F(R)h\nu)^2$ versus hν) and indirect (n=2; $(F(R)h\nu)^{1/2}$ versus hν) allowed transition modes.

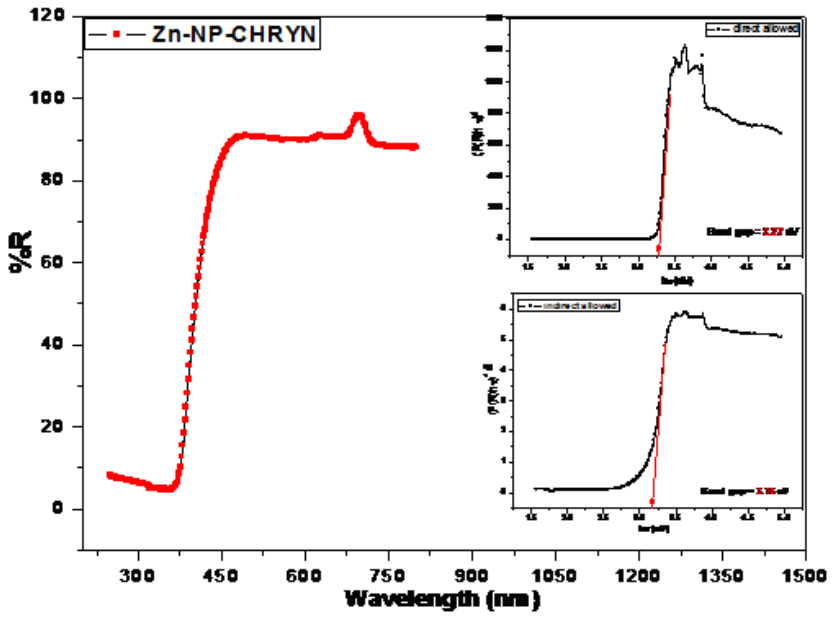

Fig. 5. Uv-visible reflection spectrum recorded for Zn-NP-CHRYN sample. Inset shows the Tauc's plot [13-15] employing Kubelka-Munk function [12] corresponding to direct (n=1/2) and indirect (n=2) allowed transition modes

The extrapolated linear portion of the curve to $F(R)=0$ provides an estimation of optical direct and indirect band gap energies equal to 3.27 eV and 3.16 eV respectively. Thus in consistent with XRD result, it is apparent that out of the two fits, the one with best fit and higher value of band gap corresponds to direct transition mode, and hence it is reasonable to infer that Zn-NP-CHRYN sample consists of hexagonal primitive lattice of Zinc (II) oxide crystalline

phase with optical direct band gap equal to 3.27 eV.

3.4. PL spectrum analysis

Figure 6 shows photoluminescence spectrum recorded for Zn-NP-CHRYN sample with an optimized excitation wavelength of 280 nm at Department of Physics, University of Kerala, Kariyavattom campus, Thiruvananthapuram, Kerala, India. There are five peaks centered at 382 nm (3.25 eV), 421 nm (2.95 eV), 451 nm (2.75 eV), 467 nm (2.66 eV), 483 nm (2.57 eV) and 493 nm (2.52 eV). This fluorescence arises due to band to band transition in nanocrystalline zinc-oxide and other defects inside the nanoparticles.

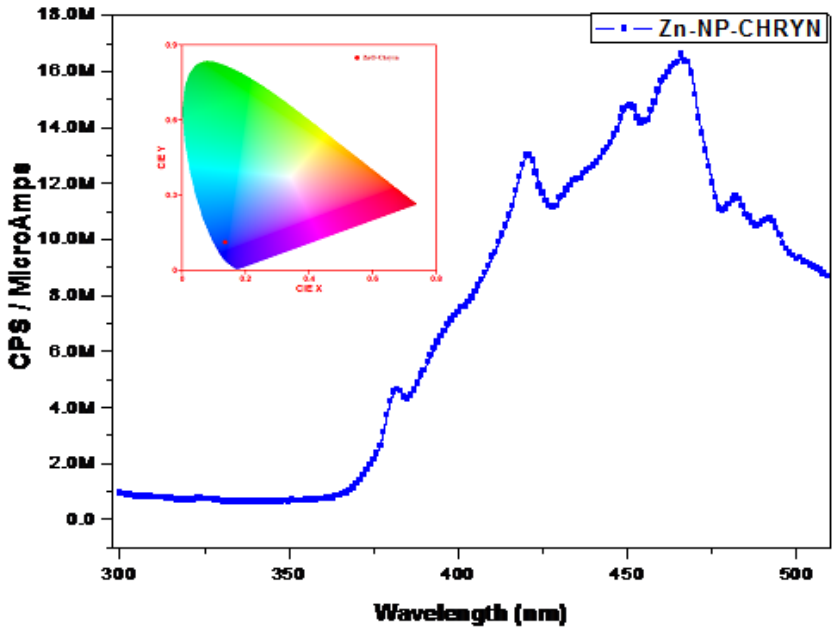

Fig. 6. PL spectrum recorded for Zn-NP-CHRYN sample. Inset shows the chromaticity diagram

Corresponding to 280 nm excitation line, the highest intensified emission peak is observed at 467 nm, which is in fact the blue light region in the visible spectrum. The emission originates from the radiative recombination of electron-hole pair [16]. Since the lamp was 280 nm uv, in order to avoid its harmonics to be emitted, the spectrum was restricted to a scan up to 530 nm. Since the optical direct band gap obtained for Zn-NP-CHRYN sample is 3.27 eV and all the said luminescence peaks have energy less than band gap, it is reasonable to infer that apart from band to band transitions, band to intermediate level or intermediate level to band transitions have been occurred. The intermediate levels might be attributed to defect induced and/or interstitial vacancy induced and/or impurity phase induced donor or accepter levels etc., in the forbidden band region in the crystal structure of zinc-oxide. Further, the color coordinates corresponding to the PL spectrum was calculated and found to be equal to (0.138, 0.113), which fall in the blue region of the chromaticity diagram as shown in the inset of figure 6. Thus it is apparent that, the prepared Zn-NP-CHRYN sample is a potential candidate for blue display applications.

4. Conclusions

Nanocrystalline hexagonal primitive lattice phase of zinc (II) oxide (ZnO) of crystallite size, 16 nm could be successfully synthesized using chrysin mediated phytochemical reduction method. From FESEM images, the coalesced aggregates of crystallites forming long needle like gain morphology could be evidenced with average size equivalent to the Debye-Scherrer crystallite size calculated from XRD pattern. Tauc' plot of uv-visible spectrum employing Kubelka-Munk function provided a direct optical band gap of 3.27 eV. The photoluminescence spectrum

and the related color coordinates estimated from chromaticity diagram revealed that for Zn-NP-CHRYN sample, the optical emission fall in the blue region of the chromaticity diagram; which prospected towards the efficacy of the material as potential candidate for display applications.

Acknowledgements

Research and Postgraduate Department of Physics (approved Research Center of University of Kerala), S.N. College, Kollam-691001, Kerala, India

References

[1] P. Visali, R. Bhuvaneswari, Optik 202 (2020)Article 163706
[2] S. D. Senol, E. Ozugurlu, L. Arda, Ceramics International, 46(615) (2020) 7033-7044
[3] Sung-Nam Kwon, Jae-Hun Yu, Seok-In Na, Journal of Alloys and Compounds,80115 (2019) 277-284
[4] Van ThaiDang Thi Tu OanhNguyen Thi HienTruong Anh ThiLe Tien DaiNguyen, Materials Today Communications, 22, (2020), 100826.
[5] Arun S. Prasad, Materials Science in Semiconductor Processing 53, (2016) 79–83.
[6] Cibin Baby, Athira Prasad, Kanchana A., Rajeswary M., Sajitha M, Praveen K.H. and Arun S. Prasad, Int. J. Adv. Research in Sci. Engg. 6 (3) (2017) 66-71.
[7] Arun S. Prasad, Materials Science in Semiconductor Processing 71 (2017) 342-347.
[8] Arun S. Prasad, Materials Science-Poland 37 (3) (2019) 503-509.
[9] Ahmad Salimi and Jalal Pourahmad in Polyphenols: Prevention and Treatment of Human Disease (Second Edition), Elsevier (2018) pp. 455-466.
[10] A. Shamsizadeh and A. Moghaddamahmadi et al., in Nutrition and Lifestyle in Neurological Autoimmune Diseases, Elsevier (2017) pp. 285-288.
[11] B.D. Cullity, Elements of X-ray Diffraction, Addison-Wesley, Reading, 1978.
[12] A. B. MurphySolar Energy Mater. Solar Cells, 91 (2007) 1326-1337.
[13] J. Tauc, R. Grigorovici, and A. Vancu, Phys. Status Solidi, 15 (1966) 627-637.
[14] J. Tauc (F. Abeles ed.), Optical Properties of Solids, North-Holland ,1972.
[15] E. A. Davis and N. F. Mott, Philos. Mag., 22 (1970) 903-922.
[16] L.Xu , G.Zheng , S.Pei and J.Wang ,Optik , 158 (2018)382-390.